

Structural Transformations of $\text{VOHPO}_4 \cdot 1/2\text{H}_2\text{O}$ in the Presence of Ammonia

Yue Zhang,* Andreas Martin, Gert-Ulrich Wolf, Stefan Rabe, Horst Worzala, and Bernhard Lücke

*Institut für Angewandte Chemie Berlin-Adlershof e.V., Rudower Chaussee 5,
D-12484 Berlin, Germany*

Manfred Meisel

*Humboldt Universität zu Berlin, Institut für Anorganische und Allgemeine Chemie,
Hessische Strasse 1-2, D-10115 Berlin, Germany*

Klaus Witke

*Bundesanstalt für Materialforschung und -prüfung, Rudower Chaussee 5,
D-12484 Berlin, Germany*

Received November 28, 1995. Revised Manuscript Received February 14, 1996[®]

The structural transformation of vanadium phosphate hemihydrate, $\text{VOHPO}_4 \cdot 1/2\text{H}_2\text{O}$, into ammonium vanadyl pyrophosphate, $(\text{NH}_4)_2[(\text{VO})_3(\text{P}_2\text{O}_7)_2]$, was studied by XRD and spectroscopic methods such as FTIR and Raman spectroscopy. The reaction was carried out at 673 K in the presence of the ammoxidation feed (toluene, oxygen (air), ammonia, and water vapor), proceeding through an intermediate crystalline phase. The main product of the transformation was $\alpha\text{-(NH}_4)_2[(\text{VO})_3(\text{P}_2\text{O}_7)_2]$, which is isostructural to $\alpha\text{-K}_2[(\text{VO})_3(\text{P}_2\text{O}_7)_2]$. Both materials are characterized by the orthorhombic space group $Pna2_1$ and an intersecting tunnel structure. Apart from $\alpha\text{-(NH}_4)_2[(\text{VO})_3(\text{P}_2\text{O}_7)_2]$, a vanadium-rich phase was formed according to the stoichiometry which is probably a mixed valent vanadium oxide. The structural transformation proceeded also in the same direction without participation of the aromatic substrate. The reaction of $\text{VOHPO}_4 \cdot 1/2\text{H}_2\text{O}$ carried out only under an ammonia/oxygen (air) flow led to the generation of $\alpha\text{-(NH}_4)_2[(\text{VO})_3(\text{P}_2\text{O}_7)_2]$ as well, but to a minor degree. An XRD-amorphous material was obtained, being the main phase. The treatment of the hemihydrate with an ammonia/nitrogen flow generated an XRD-amorphous product and a deep reduction of $\text{V}^{\text{IV}} \Rightarrow \text{V}^{\text{III}}$ proceeded.

Introduction

Knowledge of catalyst composition and structure, both at the surface and in the bulk, is crucial to a fundamental understanding of the chemistry occurring in heterogeneous catalysis and especially in the explanation of the mechanisms of catalytic processes. In redox reactions, the electronic configuration and morphology of oxide catalysts are important in determining their activities and selectivities (e.g., refs 1–3).

Recently, various vanadium phosphates (VPO) with definite framework structures were used as catalyst precursors ($\alpha\text{-VOPO}_4$, $\beta\text{-VOPO}_4$, VOHPO_4 , $\text{VOHPO}_4 \cdot 1/2\text{H}_2\text{O}$, $(\text{VO})_2\text{P}_2\text{O}_7$, and $(\text{NH}_4)_2[\text{VOP}_2\text{O}_7]$) in the ammoxidation reaction of substituted methylaromatics^{6–8} and

heteroaromatics^{7,9} to their corresponding nitriles, indicating the potential of such VPO materials for these redox reactions. Substituted aromatic nitriles are important organic intermediates for the production of dyestuffs, pharmaceuticals, pesticides, and other valuable chemical compounds (e.g., refs 4 and 5). Apart from $(\text{VO})_2\text{P}_2\text{O}_7$, all other VPO phases revealed a precursor/catalyst transformation, resulting in the generation of ammonium-containing oxovanadium(IV) as well as vanadium(III) diphosphates^{6,7} as indicated by X-ray powder diffraction (XRD).

It is well-known that $\text{VOHPO}_4 \cdot 1/2\text{H}_2\text{O}$ transforms into vanadyl pyrophosphate $(\text{VO})_2\text{P}_2\text{O}_7$ ^{10,11} in an air/*n*-butane flow above 623 K, for example. The latter VPO phase is an active and selective catalyst in the oxidation of *n*-butane to maleic anhydride (e.g., refs 12–17). Interestingly, in the ammoxidation studies it was found that

[®] Abstract published in *Advance ACS Abstracts*, April 1, 1996.

(1) Oyama, S. T.; Desikan, A. N.; Hightower, J. W. *Catalytic Selective Oxidation* Oyama, S. T., Hightower, J. W., Eds., ACS Symp. Ser.; ACS: Washington, 1993; Vol. 523, p 1.

(2) Bordes, E. *Elementary Reaction Steps in Heterogeneous Catalysis*; (Joyner, R. W., van Santen, R. A., Eds.), Kluwer Academic Press: Amsterdam, 1993; p 137.

(3) Haber, J. *Catalysis of Organic Reactions*; Kosak, J. R., Johnson, T. A., Eds.; Chemical Industries Ser., Marcel Dekker: New York, 1994; Vol. 53, p 151.

(4) Grasselli, R. K.; Burrington, J. D.; DiCosimo, R.; Friedrich, M. S.; Suresh, D.D. *Stud. Surf. Sci. Catal.* **1988**, *41*, 317.

(5) Rizayev, R. G.; Mamedov, E. A.; Vislovskii, V. P.; Sheinin, V. E. *Appl. Catal. A: Gen.* **1992**, *83*, 103.

(6) Martin, A.; Lücke, B.; Seeboth, H.; Ladwig, G.; Fischer, E. *React. Kinet. Catal. Lett.* **1989**, *38*, 33.

(7) Lücke, B.; Martin, A. *Catalysis of Organic Reactions*; Scaros, M. G., Prunier, M. L., Eds.; Chemical Industries Ser.; Marcel Dekker: New York, 1995, Vol. 62, p 479.

(8) Martin, A.; Lücke, B.; Wolf, G.-U.; Meisel, M. *Catal. Lett.* **1995**, *33*, 349.

(9) Martin, A.; Lücke, B.; Seeboth, H.; Ladwig, G. *Appl. Catal.* **1989**, *49*, 205.

(10) Johnson, J. W.; Johnston, D. C.; Jacobson, A. J.; Brody, J. F. *J. Am. Chem. Soc.* **1984**, *106*, 8123.

(11) Bordes, E. *Catal. Today* **1987**, *1*, 499.

VOHPO₄·¹/₂H₂O was transformed into the ammonium vanadyl pyrophosphate (NH₄)₂[(VO)₃(P₂O₇)₂]^{6,8} during the heating of the precursor under ammoxidation feed. The ammoxidation feed was passed over the precursor at lower temperatures than those necessary for the dehydration into pyrophosphate to avoid a transformation in such direction. The precursor transformation was finished within ca. 4 h under the reaction conditions applied (reaction temperature up to 723 K). The transformation product was identified first by comparison with the XRD patterns of synthesized (NH₄)₂[(VO)₃(P₂O₇)₂]¹⁸ and K₂[(VO)₃(P₂O₇)₂].¹⁸

The purpose of this current research is to explore the structural transformation of VOHPO₄·¹/₂H₂O precursor compound upon the ammoxidation of methylaromatics, e.g., toluene. Furthermore, VOHPO₄·¹/₂H₂O was exposed to single-feed components such as ammonia/oxygen (air)/water vapor, ammonia/oxygen (air), and ammonia/nitrogen mixtures in order to get further information about the role of the single-feed components in the transformation process. The paper reports the results of XRD studies as well as FTIR and Raman spectroscopic investigations corresponding to the particular interactions/reactions.

Experimental Section

The synthesis procedure of VOHPO₄·¹/₂H₂O has been previously reported, using an aqueous medium.^{19,20} (NH₄)₂[(VO)₃(P₂O₇)₂] was prepared by heating a mixture, containing V₂O₅ (0.055 mol), (NH₄)₂HPO₄ (0.88 mol), and a small amount of inoculating crystals at 598 K for 2.5 h in air. A light green powder was obtained after the raw sample had been eluted with water and dried in air (described below as the α-phase).¹⁸ The valence state of the vanadium was determined by potentiometric titration using a modified method of Niwa and Murakami.^{21,22} The H:N and the N:V ratios of the synthesized sample amounted to 4.02 and 0.67, respectively. These values are in good agreement with the theoretical ones.

In general, the samples used in the present work were prepared by treatment of VOHPO₄·¹/₂H₂O (500 mg each) with (a) ammoxidation feed, (b) ammonia/oxygen (air)/water vapor, (c) ammonia/oxygen (air), and (d) ammonia/nitrogen at 673 K for several times and subsequently cooling to room temperature under nitrogen. Every sample was heated temperature-programmed (heating rate β = 10 K/min), first under nitrogen up to 393 K, above 393 K nitrogen was replaced by the different feed mixtures (a–d). Sample description, reaction conditions, and reaction times are summarized in Table 1. Table 2 gives a survey on the results of the chemical analysis (V, N, H) of all samples as well as their vanadium valence state determined as described above. Furthermore, a small amount of a catalyst used in a long-term ammoxidation

Table 1. Sample Description and Reaction Conditions of Sample Preparation

sample	reaction time (h)	reaction conditions
VP _{a0}	a	NH ₃ :toluene:air:H ₂ O = 1:0.22:6.95:5.29
VP _{a0.25}	0.25	
VP _{a0.5}	0.5	
VP _{a1}	1	
VP _{a2}	2	
VP _{a3}	3	
VP _{a6}	6	NH ₃ :air:H ₂ O = 1:6.96:5.43
VP _{a10}	10	
VP _{b1}	1	
VP _{b3}	3	NH ₃ :air = 1:6.96
VP _{b8}	8	
VP _{c1}	1	
VP _{c3}	3	NH ₃ :N ₂ = 1:6.96
VP _{c8}	8	
VP _{d1}	1	
VP _{d3}	3	8
VP _{d8}	8	

^a Heated to 673 K and cooled to room temperature under N₂ immediately.

experiment was taken from the reactor after 120 h on-stream in order to look for possible phase changes by means of XRD.

X-ray diffraction patterns of all samples described above were recorded with a Stoe automatic transmission powder diffractometer (STADIP) using Cu Kα₁ radiation equipped with a Ge monochromator and a linear position-sensitive detector. Additionally, samples VP_{a1}, VP_{a2}, VP_{a3}, VP_{a6}, and VP_{a10} were mixed with 10 wt % silicon. The integrated peak area of the (111)-reflection of Si at 28.443° 2θ was used as internal standard for comparison with integrated peak areas of the compounds under consideration. The unit cell parameters of (NH₄)₂[(VO)₃(P₂O₇)₂] were determined using programs of the Stoe diffractometer software system.²³

The Raman spectra were recorded with a DILOR-XY spectrometer equipped with a nitrogen-cooled ccd camera as the detector. The samples were excited using the 514.5 nm line from a Carl Zeiss ILA 120 argon ion laser with power levels up to 66 mW incident into the entrance optics (1 mW = 0.4 kW/cm² at the sample). Backscattering geometry of the micro-Raman technique (×10) was used to record spectra of the powder samples.

The infrared spectra were obtained with a Bruker IFS 66 FTIR spectrophotometer, with 2 mg of sample powder each diluted in 400 mg of KBr and pressed into 20 mm o.d. wafer. For each spectrum 100 scans were accumulated at 2 cm⁻¹ resolution.

Results

X-ray Diffraction. Figure 1 shows the XRD patterns of the hemihydrate precursor, the samples obtained after interaction of VOHPO₄·¹/₂H₂O with the ammoxidation feed at 673 K for several times (VP_{a0}–VP_{a10}, run a) and the as-synthesized (NH₄)₂[(VO)₃(P₂O₇)₂]. The transformation proceeded through an intermediate phase, appearing after 15 min on-stream (sample VP_{a0.25}). Simultaneously, the reflections of (NH₄)₂[(VO)₃(P₂O₇)₂] appeared whereas the reflections of VOHPO₄·¹/₂H₂O almost disappeared after 1 h on-stream (sample VP_{a1}).

Figure 2 depicts the XRD patterns of the catalyst sample taken from the long-term experiment, running for 120 h under ammoxidation conditions and the as-synthesized (NH₄)₂[(VO)₃(P₂O₇)₂]. It is evident that the

(12) Bordes, E.; Courtine, P. *J. Chem. Soc., Chem. Commun.* **1985**, 296.

(13) Centi, G.; Trifirò, F.; Ebner, J. F.; Franchetti, V. M. *Chem. Rev.* **1988**, *88*, 55.

(14) Centi, G. *Catal. Today* **1993**, *16*, 5.

(15) Okuhara, T.; Inumaru, K.; Misono, M. *Catalytic Selective Oxidation*; Oyama, S. T., Hightower, J. W., Eds.; ACS Symp. Ser.; ACS: Washington, 1993; Vol. 523, p 156.

(16) Zhang-Lin, Y.; Forissier, M.; Sneed, R. P.; Védrine, J. C.; Volta, J. C. *J. Catal.* **1994**, *145*, 256.

(17) Zhang-Lin, Y.; Forissier, M.; Védrine, J. C.; Volta, J. C. *J. Catal.* **1994**, *145*, 267.

(18) Schlesinger, K., late, 1983, draft of dissertation.

(19) Schlesinger, K.; Ladwig, G.; Meisel, M.; Kubias, B.; Weinberger, R.; Seeboth, H., 1984, *DP-WP 256.659*.

(20) Berndt, H.; Büker, K.; Martin, A.; Brückner, A.; Lücke, B. *J. Chem. Soc., Faraday Trans.* **1995**, *91*, 725.

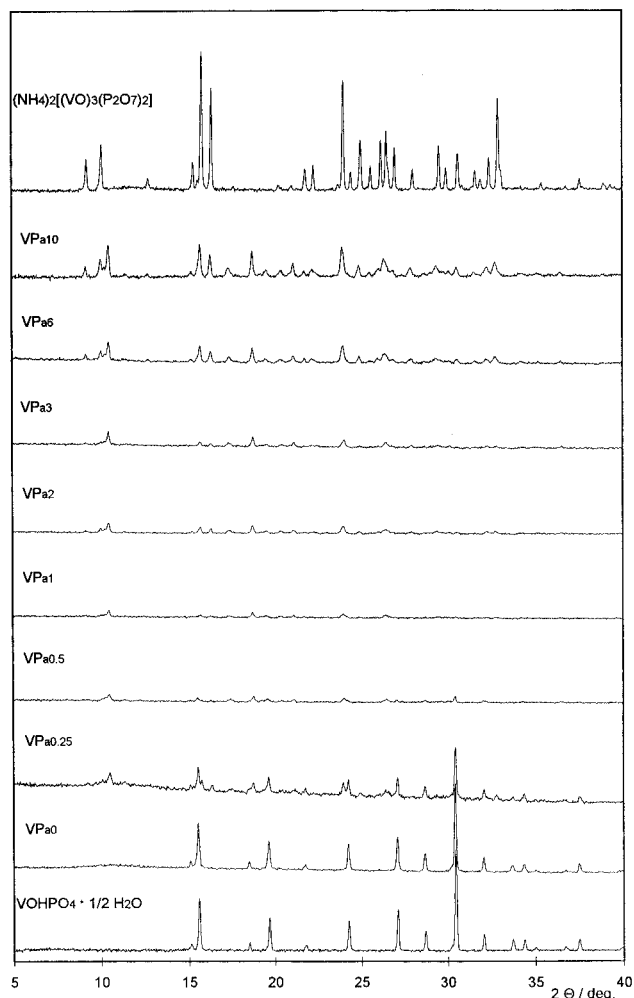
(21) Niwa, M.; Murakami, Y. *J. Catal.* **1982**, *76*, 9.

(22) Kubias, B.; Meisel, M.; Wolf, G.-U.; Rodemerck, U. *Stud. Surf. Sci. Catal.* **1994**, *82*, 195.

(23) Worzala, H.; Calov, U.; Wolf, G.-U. *Powder Diffraction File*, 1996, Set 46.

Table 2. Chemical Analysis of the Samples and Their Vanadium Valence State

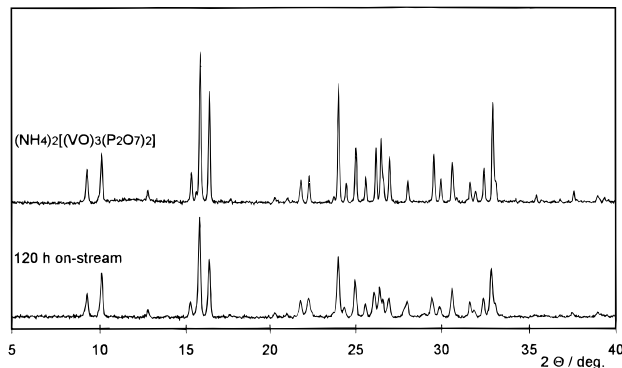
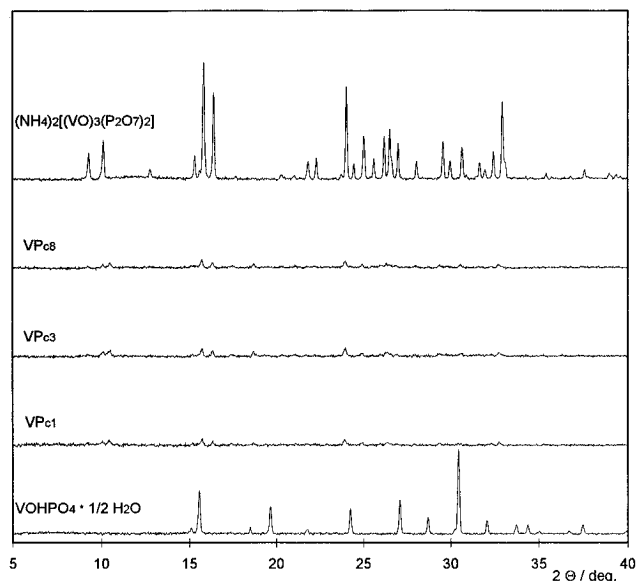
sample	V/wt %	N/wt %	H/wt %	V/N ratio	H/N ratio	V valence state
VP _{a0}	29.72	1.14	1.22	7.19	15.06	4.024
VP _{a0.25}	30.11	2.89	1.13	2.87	5.49	4.106
VP _{a0.5}	29.80	3.26	1.26	2.51	5.41	4.133
VP _{a1}	30.62	3.93	1.11	2.14	3.95	4.118
VP _{a2}	30.16	4.26	1.18	1.94	3.88	4.109
VP _{a3}	30.49	4.17	1.16	2.01	3.89	4.104
VP _{a6}	30.44	4.42	1.22	1.89	3.86	4.107
VP _{a10}	30.04	4.46	1.18	1.85	3.70	4.108
VP _{b1}	30.09	4.21	1.16	1.96	3.85	4.112
VP _b	29.69	4.60	1.25	1.77	3.81	4.116
VP _{b8}	28.87	5.43	1.47	1.46	3.79	4.164
VP _{c1}	30.82	4.19	0.84	2.02	2.81	4.064
VP _{c3}	30.59	4.13	0.86	2.03	2.92	4.062
VP _{c8}	30.32	4.46	0.88	1.87	2.76	4.056
VP _{d1}	31.12	3.14	1.07	2.72	4.78	3.922
VP _{d3}	31.26	3.12	0.91	2.75	4.08	3.862
VP _{d8}	31.84	3.65	0.96	2.39	3.68	3.764

**Figure 1.** X-ray powder diffraction patterns of $\text{VOHPO}_4 \cdot 1/2\text{H}_2\text{O}$, hemihydrate samples treated with ammoxidation gas flow (VP_{a0}–VP_{a10}, run a) and the as-synthesized $(\text{NH}_4)_2[(\text{VO})_3(\text{P}_2\text{O}_7)_2]$.

XRD pattern of the sample is in good agreement with that of the synthesized material with a comparable crystallinity.

The same procedure carried out in the absence of the aromatic substrate (run b) led to the exact same results, i.e., the formation of $(\text{NH}_4)_2[(\text{VO})_3(\text{P}_2\text{O}_7)_2]$.

Figure 3 depicts the XRD patterns of $\text{VOHPO}_4 \cdot 1/2\text{H}_2\text{O}$, the samples VP_{c1}–VP_{c8} obtained after reaction with an

**Figure 2.** X-ray powder diffraction patterns of an ammoxidation catalyst ($\text{VOHPO}_4 \cdot 1/2\text{H}_2\text{O}$ precursor) proceeding 120 h on-stream in comparison to the as-synthesized $(\text{NH}_4)_2[(\text{VO})_3(\text{P}_2\text{O}_7)_2]$.**Figure 3.** X-ray powder diffraction patterns of $\text{VOHPO}_4 \cdot 1/2\text{H}_2\text{O}$, hemihydrate samples treated with an ammonia/air gas flow (VP_{c1}–VP_{c8}, run c) and the as-synthesized $(\text{NH}_4)_2[(\text{VO})_3(\text{P}_2\text{O}_7)_2]$.

ammonia/oxygen (air) flow in the absence of water vapor at 673 K for different times (run c) and the synthesized $(\text{NH}_4)_2[(\text{VO})_3(\text{P}_2\text{O}_7)_2]$ sample. The patterns of the samples VP_{c1}, VP_{c3}, and VP_{c8} revealed the generation of $(\text{NH}_4)_2[(\text{VO})_3(\text{P}_2\text{O}_7)_2]$ as well, but only to a minor extent with poor crystallinity in comparison to that of

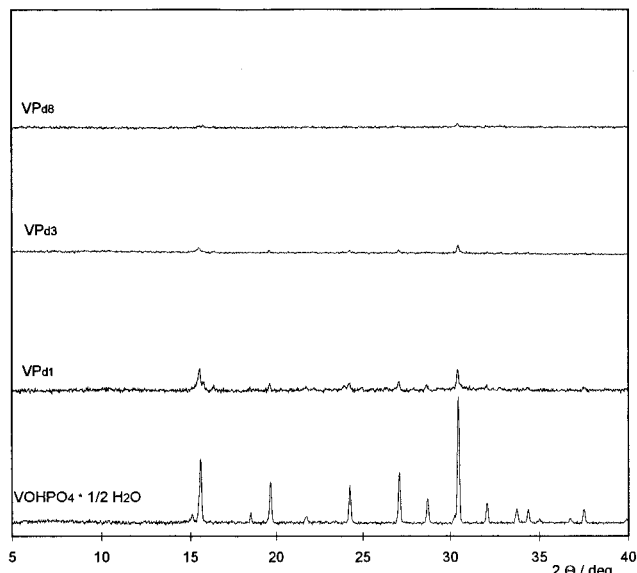


Figure 4. X-ray powder diffraction patterns of $\text{VOHPO}_4 \cdot \frac{1}{2}\text{H}_2\text{O}$ and the hemihydrate samples treated with an ammonia/nitrogen gas flow ($\text{VP}_{\text{d}1}$ – $\text{VP}_{\text{d}8}$, run d).

samples obtained by runs (a) and (b) with additional feeding of water.

Figure 4 demonstrates the XRD patterns of the hemihydrate and the samples obtained ($\text{VP}_{\text{d}1}$ – $\text{VP}_{\text{d}8}$) after the reaction with an ammonia/nitrogen flow (run d). The patterns depict the progressive formation of an XRD-amorphous product.

It must be noted here that all recorded XRD patterns reveal some reflections not belonging to $(\text{NH}_4)_2[(\text{VO})_3(\text{P}_2\text{O}_7)_2]$, especially at larger angles. These reflections could not be assigned to another known phase up to now.

Raman Spectroscopy. Laser Raman spectroscopy was often applied to study catalyst surfaces that contain vanadium (e.g., refs 24–27) and are proven effective in describing the structure of the catalysts discussed. In the present work Raman spectroscopy was used to support the findings on the structural transformations of the hemihydrate precursor under ammoxidation conditions. The Raman spectra of $\text{VOHPO}_4 \cdot \frac{1}{2}\text{H}_2\text{O}$, the synthesized $(\text{NH}_4)_2[(\text{VO})_3(\text{P}_2\text{O}_7)_2]$, and sample $\text{VP}_{\text{a}10}$ are presented in Figure 5. $\text{VOHPO}_4 \cdot \frac{1}{2}\text{H}_2\text{O}$ (spectrum a) exhibits a strong Raman band at ca. 985 cm^{-1} due to $\nu(\text{V}=\text{O})$ stretching vibration (e.g., ref 28). The spectrum of the as-synthesized $(\text{NH}_4)_2[(\text{VO})_3(\text{P}_2\text{O}_7)_2]$ (spectrum b) shows a band at ca. 977 cm^{-1} that is also attributed to the stretching vibrations of $\text{V}=\text{O}$ groups. The strong band at ca. 914 cm^{-1} can be assigned to the asymmetric vibration of pyrophosphate units, for instance, as recently reported by real-time in situ Raman spectroscopic investigations of $\text{VOHPO}_4 \cdot \frac{1}{2}\text{H}_2\text{O}$ transformation to $(\text{VO})_2\text{P}_2\text{O}_7$.²⁷ The Raman spectrum of the sample $\text{VP}_{\text{a}10}$ (spectrum c) is very similar to that of $(\text{NH}_4)_2[(\text{VO})_3(\text{P}_2\text{O}_7)_2]$. However, a weak feature near 860 cm^{-1}

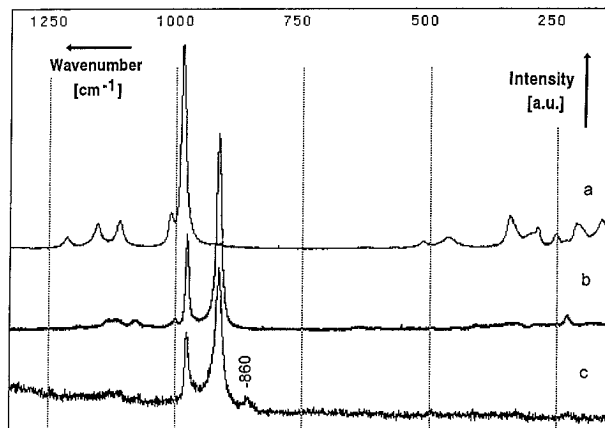


Figure 5. Raman spectra of $\text{VOHPO}_4 \cdot \frac{1}{2}\text{H}_2\text{O}$ (a), sample $\text{VP}_{\text{a}10}$ (b), and the as-synthesized $\alpha\text{-}(\text{NH}_4)_2[(\text{VO})_3(\text{P}_2\text{O}_7)_2]$ (c).

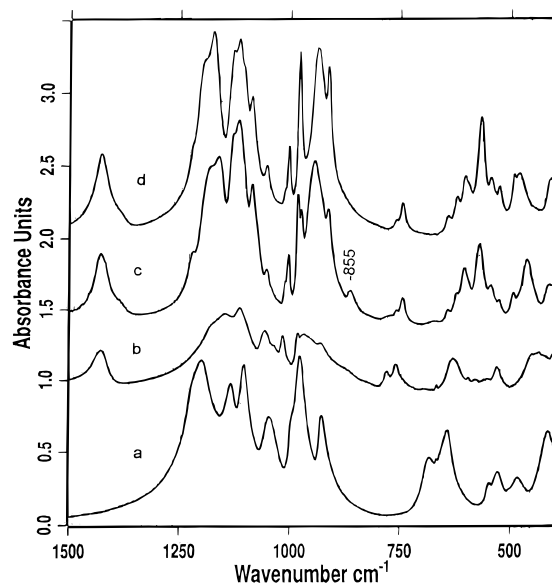


Figure 6. Infrared spectra of $\text{VOHPO}_4 \cdot \frac{1}{2}\text{H}_2\text{O}$ (a), samples $\text{VP}_{\text{a}6}$ (b), and $\text{VP}_{\text{a}10}$ (c), and the as-synthesized $\alpha\text{-}(\text{NH}_4)_2[(\text{VO})_3(\text{P}_2\text{O}_7)_2]$ (d).

distinctly occurs in the spectrum of the sample $\text{VP}_{\text{a}10}$, but it is absent in the spectrum of $(\text{NH}_4)_2[(\text{VO})_3(\text{P}_2\text{O}_7)_2]$. Bands at ca. 860 cm^{-1} are probably attributed to the stretches of $\text{V}-\text{O}$ (e.g., ref 24).

FTIR Spectroscopy. The infrared absorptions for VPO compounds occurring in the region $1500\text{--}400\text{ cm}^{-1}$ are ascribed to framework vibrations, being sensitive to changes of structure. Figure 6 shows the infrared spectra of $\text{VOHPO}_4 \cdot \frac{1}{2}\text{H}_2\text{O}$, the samples $\text{VP}_{\text{a}6}$ and $\text{VP}_{\text{a}10}$ as well as the synthesized $(\text{NH}_4)_2[(\text{VO})_3(\text{P}_2\text{O}_7)_2]$. As expected, the spectrum of sample $\text{VP}_{\text{a}10}$ is identical, and that of sample $\text{VP}_{\text{a}6}$ is in many ways similar, to the spectrum of $(\text{NH}_4)_2[(\text{VO})_3(\text{P}_2\text{O}_7)_2]$. In the spectrum of the sample $\text{VP}_{\text{a}10}$, a single peak at 855 cm^{-1} is evident as well, which is absent in the spectra of other VPO compounds. This observation corresponds to the Raman investigations.

Discussion

It is well-known that $\text{VOHPO}_4 \cdot \frac{1}{2}\text{H}_2\text{O}$ undergoes a topotactic reaction to $(\text{VO})_2\text{P}_2\text{O}_7$.^{10,11,29} From recent XRD studies,^{30,31} it was found that the structural

(24) Hardcastle, F. D.; Wachs, I. E. *J. Phys. Chem.* **1992**, *95*, 5031.

(25) Gao, X.; Ruiz, P.; Xin, Q.; Guo, X.; Delmon, B. *J. Catal.* **1994**, *148*, 56.

(26) Abdelouahab, B.; Olier, R.; Guilhaume, N.; Lefebvre, F.; Volta, J.-C. *J. Catal.* **1992**, *134*, 151.

(27) Hutchings, G. J.; Desmartin-Chomel, A.; Olier, R.; Volta, J.-C. *Nature* **1994**, *368*, 41.

(28) Scharf, U.; Schneider, M.; Baiker, A.; Wokaun, A. *J. Catal.* **1994**, *149*, 344.

(29) Bordes, E.; Courtine, P. *J. Solid State Chem.* **1984**, *55*, 270.

transformation from $\text{VOHPO}_4 \cdot 1/2\text{H}_2\text{O}$ into $(\text{VO})_2\text{P}_2\text{O}_7$ proceeds through a state with an extensive degree of disorder. In the present work, evidence is also given for the existence of a low crystalline intermediate state, appearing immediately after the beginning of the structural transformation of the hemihydrate. Such material could be formed in this case by penetration of ammonia into the layers of $\text{VOHPO}_4 \cdot 1/2\text{H}_2\text{O}$, possibly accompanied by a break of V–O–P bonds, also generating ammonium ions.²⁰ Shirai et al.³² also described a structural change from V=O to V–OH during interaction of ammonia and supported vanadium oxide, generating additional ammonium ions. These processes are promoted by the interaction of the solid material with water vapor, causing the generation of –OH groups to a great extent.³³ Additionally, the water fed in excess avoids the commonly proceeding dehydration from $\text{VOHPO}_4 \cdot 1/2\text{H}_2\text{O}$ into $(\text{VO})_2\text{P}_2\text{O}_7$ because of a shift of the dehydration equilibrium to the hemihydrate. Furthermore, it seems that the interaction between ammonia and P–OH groups could partially prevent the fast condensation of P–OH groups between the layers as well. The presence of oxygen stabilizes the vanadium oxidation state +4, while the absence of oxygen in the reaction leads to a progressive generation of V^{III} as described below and in ref 20.

In addition, a result of the penetration of ammonia into the hemihydrate layers in the sense of a VPO intercalation compound^{34–36} could be the subsequent generation of a layered intermediate structure.³⁷ It seems that the mobility of P–O– units in such a layered, water vapor “flooded” and softened structure could lead to the formation of new, crystalline ammonium ions-containing structures. Similar mechanisms were discussed for other phosphate systems.³⁸

In contrast, the reaction carried out in the absence of water vapor seems to proceed mainly to an XRD-amorphous product whereas $(\text{NH}_4)_2[(\text{VO})_3(\text{P}_2\text{O}_7)_2]$ was generated only in a minor amount. Therefore, it was not surprising to find an almost constant vanadium valence state of ca. 4.05 and an H/N ratio of ca. 3. The latter suggests a dissociatively initiated reaction of ammonia (nucleophilic attack of ammonia, ammonolysis) and V–O–P and/or possibly generated P–O–P links to form V/P–O– NH_4 and V/P– NH_2 groups as proposed by Matsuura.³⁹ Thus, it seems that a defined water concentration, depending on the transformation conditions, is necessary for the formation of the NH_4^+ ions-containing phase. Lower concentrations of water, fed or formed by oxidoreductive interactions as well as condensation reactions (e.g., run c), seem to be sufficient for the generation of only a relatively small amount of

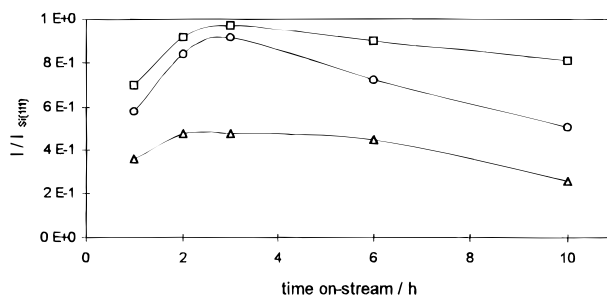


Figure 7. Intensity ratios of the main reflections of the intermediate phase to the silicon (111) reflex ($2\theta = 28.430$) used as internal standard vs time on-stream (intermediate phase reflections: □, $2\theta = 10.5$; ○, $2\theta = 17.4$; △, $2\theta = 18.7$).

ammonium ions, i.e., a small amount of $(\text{NH}_4)_2[(\text{VO})_3(\text{P}_2\text{O}_7)_2]$. Finally, the reaction with the ammonia/nitrogen flow (run d) led to a partial reduction of $\text{V}^{\text{IV}} \rightarrow \text{V}^{\text{III}}$, depending on reaction time and temperature as shown by the determined vanadium valence states (see Table 2). Similar results were obtained by the interaction of $(\text{VO})_2\text{P}_2\text{O}_7$ with an ammonia/helium flow at elevated temperatures.²⁰

Furthermore, it seems that during the precursor transformation under ammoxidation conditions (run a) simultaneously with the generation of the metastable phase the stable final product of the transformation appears. This implies a relatively fast formation of the metastable phase that transforms slower into the $(\text{NH}_4)_2[(\text{VO})_3(\text{P}_2\text{O}_7)_2]$. However, the reflections of $\text{VOHPO}_4 \cdot 1/2\text{H}_2\text{O}$ completely disappeared after 60 min on-stream and the ones of $(\text{NH}_4)_2[(\text{VO})_3(\text{P}_2\text{O}_7)_2]$ and of the intermediate phase rise. The proof of the metastable character of the intermediate phase is demonstrated in Figure 7, showing intensity ratios of the main reflections of this phase to the reflex of the (111) plane of the Si internal standard material. Evidently, the intensity of main reflections run through a maximum passed at ca. 3 h on-stream. The same investigations show a slow but distinct increase of the reflections of $(\text{NH}_4)_2[(\text{VO})_3(\text{P}_2\text{O}_7)_2]$.

The reflections of $(\text{NH}_4)_2[(\text{VO})_3(\text{P}_2\text{O}_7)_2]$ generated from $\text{VOHPO}_4 \cdot 1/2\text{H}_2\text{O}$ have the same positions and intensities as those obtained for the directly synthesized $(\text{NH}_4)_2[(\text{VO})_3(\text{P}_2\text{O}_7)_2]$. The comparison of the unit-cell parameters of the NH_4^+ -containing phase with the corresponding values of $\text{K}_2[(\text{VO})_3(\text{P}_2\text{O}_7)_2]$ reported by Leclaire et al.⁴⁰ shows that both compounds are isostructural (Table 3). Thus, the formed $(\text{NH}_4)_2[(\text{VO})_3(\text{P}_2\text{O}_7)_2]$ and the isostructural K^+ -containing salt should be attributed to the α phase characterized by an orthorhombic structure, the space group $Pna2_1$ and an intersecting tunnel structure.^{40,42} The X-ray pattern of the intermediate layerlike phase demonstrates some similarities with the pattern of $\beta\text{-K}_2[(\text{VO})_3(\text{P}_2\text{O}_7)_2]$,⁴³ the high-temperature modification of $\alpha\text{-K}_2[(\text{VO})_3(\text{P}_2\text{O}_7)_2]$, having a layered structure as well.

(30) Cornaglia, L. M.; Caspani, C.; Lombardo, E. A. *Appl. Catal.* **1991**, *74*, 15.

(31) Cavani, F.; Trifirò, F. *Scientific Bases for the Preparation of Heterogeneous Catalysts*, Preprints of 6th Int. Symposium, Louvain-la-Neuve/Belgium, Sep 5–8, 1994; Vol. 1, p 1.

(32) Shirai, M.; Asakura, K.; Iwasawa, Y. *Catal. Lett.* **1994**, *26*, 229.

(33) Jahan, I.; Kung, H. H.; *Catalysis of Organic Reactions*; Kosak, J. R., Johnson, T. A., Eds.; Chemical Industries Ser.; Marcel Dekker: New York, 1994, Vol. 53, p 491.

(34) Johnson, J. W.; Jacobson, A. J.; Brody, J. F.; Rich, S. M. *Inorg. Chem.* **1982**, *21*, 3820.

(35) Gulians, V. V.; Benziger, J. B.; Sundaresan, S. *Chem. Mater.* **1994**, *6*, 353.

(36) Datta, A.; Kelkar, R. Y.; Sable, A. R. *J. Chem. Soc., Dalton Trans.* **1994**, 2145.

(37) Benabdelouahab, F.; Volta, J.-C.; Olier, R. J.-C. *J. Catal.* **1994**, *148*, 334.

(38) Worzala, H. Dissertation B, Berlin, 1985.

(39) Matsuura, I. *Stud. Surf. Sci. Catal.* **1992**, *72*, 247.

(40) Leclaire, A.; Chahboun, H.; Groult, D.; Raveau, B. *J. Solid State Chem.* **1988**, *77*, 170.

(41) Lii, K. H.; Wang, Y. P.; Cheng, C. Y.; Wang, S. L.; Ku, H. C. *J. Chin. Chem. Soc. (Taipei)* **1990**, *37*, 141.

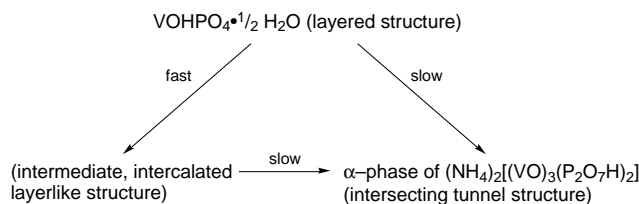
(42) Lii, K. H.; Wang, Y. P.; Wang, S. L. *J. Solid State Chem.* **1989**, *80*, 127.

(43) Lii, K. H.; Tsai, H. J.; Wang, S. L. *J. Solid State Chem.* **1990**, *87*, 396.

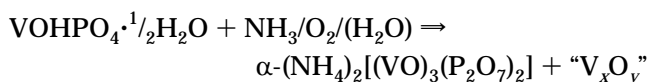
Table 3. Comparison of the Crystal Data of $M^I_2[(VO)_3(P_2O_7)_2]$ with $M^I = NH_4, K, Rb, Cs$

	$(NH_4)_2[(VO)_3(P_2O_7)_2]^{23}$	$K_2[(VO)_3(P_2O_7)_2]^{40}$	$Rb_2[(VO)_3(P_2O_7)_2]^{41}$	$Cs_2[(VO)_3(P_2O_7)_2]^{42}$
crystal system	orthorhombic	orthorhombic	orthorhombic	orthorhombic
space group	$Pna2_1$	$Pna2_1$	$Pnam$	$Pnam$
a [Å]	17.498	17.407	17.502	17.613
b [Å]	11.365	11.344	11.399	11.600
c [Å]	7.277	7.296	7.292	7.328
vol. [Å ³]	1447.2	1440.8	1454.8	1497.2
no. of formula units	4	4	4	4

The following scheme shows the possible paths of the transformation:



Evidently, some other vanadium-rich compounds must be formed, accompanying the formation of α - $(NH_4)_2[(VO)_3(P_2O_7)_2]$, because of the different V/P ratios of the precursor (1:1) and the identified transformation product (3:4) as shown in the following scheme:



The " V_xO_y " phase should contain a quarter of the total vanadium but the XRD patterns of several transformation products formed during the ammoxidation reaction do not reveal any other crystalline phase except that of α - $(NH_4)_2[(VO)_3(P_2O_7)_2]$. The potentiometric titration shows a vanadium valence state of ca. 4.1 for the materials transformed under ammoxidation conditions (run a) and in the absence of the aromatic substrate (run b), respectively. Thus, ca. 10% of the vanadium of these samples is in the valence state +5 in contrast to the synthesized α - $(NH_4)_2[(VO)_3(P_2O_7)_2]$, having only vanadium in the oxidation state +4. From this point of view it seems very likely that an XRD-amorphous phase is present as a mixed-valent vanadium oxide generated by migration of P–O– units as described above. Raman and FTIR spectra do not give more information on the nature of the additional phase (small IR and Raman bands at ca. 860–855 cm^{-1} , respectively), although several vanadium compounds present some bands in this region.

Moreover, it seems that α - $(NH_4)_2[(VO)_3(P_2O_7)_2]$ could act as a kind of support or matrix for a highly dispersed XRD-amorphous phase as suggested by Morishige et al.,⁴⁴ being an amorphous vanadium phosphate phase embedded in a crystalline phase of $(VO)_2P_2O_7$. It could

be also conceivable that the additional phase formed in our investigations is mainly involved in the N-insertion step as well as in the catalytic redox cycle, as proposed for instance by Koyano et al.⁴⁵ for the X_1 phase, existing on the surface of $(VO)_2P_2O_7$ during the catalytic oxidation of *n*-butane. These ideas are helpful to understand the distinct differences in catalytic activities and product selectivities of the synthetic α - $(NH_4)_2[(VO)_3(P_2O_7)_2]$ and the hemihydrate transformation product.⁴⁶

Conclusion

The structural transformation of $VOHPO_4 \cdot \frac{1}{2} H_2O$ carried out under ammoxidation conditions is a complicated solid-state reaction, proceeding to α - $(NH_4)_2[(VO)_3(P_2O_7)_2]$. The transformation passes through a state characterized by a softening of the hemihydrate structure by the water vapor fed. Furthermore, the penetration of ammonia into the weakened hemihydrate layers destroys the hemihydrate structure and leads to the generation of a metastable intermediate crystalline phase that has probably a layered structure as well. These interactions prevent the dehydration of the hemihydrate into $(VO)_2P_2O_7$. It seems that the generation of the metastable phase proceeds faster compared to the development of α - $(NH_4)_2[(VO)_3(P_2O_7)_2]$. The formation of the intermediate phase passes a maximum after 3 h on-stream under the applied conditions. The transformation proceeds also in the absence of the aromatic substrate. The reaction of $VOHPO_4 \cdot \frac{1}{2} H_2O$ to α - $(NH_4)_2[(VO)_3(P_2O_7)_2]$ under ammonia/oxygen (air) atmosphere occurs only to a minor extent, i.e., the presence of a sufficient concentration of water vapor seems to be necessary for the transformation. The reaction of the hemihydrate with an ammonia/nitrogen flow produces an XRD-amorphous product generated in a redox reaction, forming progressively vanadium in the oxidation state +III.

Acknowledgment. The authors thank Mrs. H. French for experimental assistance. Financial support by the Bundesministerium für Bildung, Wissenschaft, Forschung und Technologie (grant no. 03D0001B0) is gratefully acknowledged.

CM950557R

(44) Morishige, H.; Tamaki, J.; Miura, N.; Yamazoe, N. *Chem. Lett.* **1990**, 1513.

(45) Koyano, G.; Okuhara, T.; Misono, M. *Catal. Lett.* **1995**, *32*, 205.

(46) Martin, A.; Lücke, B.; Meisel, M. *Catal. Lett.*, in press.